

Original Article

***In Vivo* Imaging of Renal Redox Status during Azelnidipine Treatment**

Aki HIRAYAMA¹, Atsushi UEDA², Takaaki OTEKI³, Sohji NAGASE⁴,
Kazumasa AOYAGI¹, and Akio KOYAMA⁵

The effect of the calcium channel blocker azelnidipine on the redox status of a murine hypertension model was analyzed and imaged using *in vivo* low frequency electron paramagnetic resonance (EPR). A murine two kidney–one clip (2K1C) hypertension model was produced by a clipping of the right renal artery. The resulting hypertensive mice were treated with low-dose azelnidipine (1 mg/kg/d), with high-dose azelnidipine (3 mg/kg/d) or without azelnidipine (HT group). An EPR system equipped with a loop-gap resonator and an imaging system was employed. Redox status was evaluated as organ reducing activity measured by means of the decay rate (half-lives) of the spin probe 3-carbamoyl-2,2,5,5-tetramethylpyrrolidine-1-oxyl (Carbamoyl-PROXYL). Four weeks after clipping the mice demonstrated hypertension as expected. After the additional 2 weeks of azelnidipine treatments, the Carbamoyl-PROXYL half-lives of the Low and High azelnidipine groups measured in the upper abdominal area were significantly shorter than those of the HT group, suggesting improvements in the reducing activity. The blood pressures of the three groups showed no significant differences at this time, and there was no correlation between the renal reducing activity and either blood pressure or serum creatinine values. EPR imaging studies revealed that the improvement in abdominal reducing activity was mainly recognized in the kidney but not in the liver. These results indicate that azelnidipine ameliorates renal redox status through an improvement in reducing activity independent of blood pressure control. (*Hypertens Res* 2008; 31: 1643–1650)

Key Words: oxidative stress, imaging, azelnidipine, electron paramagnetic resonance

Introduction

A constant stream of studies alleged an important role of reactive oxygen species (ROS), especially superoxide anion ($O_2^{\cdot-}$), in the pathogenesis of hypertension. As this allegation become more widely recognized, the importance of analyzing the kinetics of ROS or related substances *in vivo* has increased. However, it is still difficult to measure the concurrent *in vivo* redox status non-invasively because ROS related reactions generally have high rate constants and they are often

estimated indirectly by measuring the end-products of lipid, protein or gene oxidation. Inevitably, problems concerning the resemblance to and reproduction of *in vivo* circumstances are continuously open to criticism in these *in vitro* or *ex vivo* estimations (1). In the field of hypertension research, these problems make it difficult to distinguish the antioxidative effects of the drugs from their effects on blood pressure or hemodynamics (2, 3).

Electron paramagnetic resonance (EPR) has the potential for *in vivo* direct measurement of redox status. Applications of EPR for *in vivo* measurements has been difficult because 1)

From the ¹Center for Integrative Medicine, Tsukuba University of Technology, Tsukuba, Japan; ²Department of Nephrology, Namegata District General Hospital, Namegata, Japan; ³Center for Clinical Medicine and Research, International University of Health and Welfare, Nasushiobara, Japan; ⁴Nagase Naika Clinic, Moriya, Japan; and ⁵Ibaraki Prefectural University of Health Sciences, Ibaraki, Japan.

This study was supported by a Grant-in-Aid for Scientific Research from the Japan Society for the Promotion of Science (#18590878).

Address for Reprints: Aki Hirayama, M.D., Ph.D., Integrated Medical Center, Tsukuba University of Technology, 4–12–7 Kasuga, Tsukuba 305–8521, Japan. E-mail: aki-hira@k.tsukuba-tech.ac.jp

Received December 25, 2007; Accepted in revised form April 27, 2008.

the absolute concentration of biological radicals in a steady condition is quite low and 2) microwaves used in the conventional X-band EPR system causes dielectric loss by body fluid. The recent development of a nitroxyl radical-spin probe method and low-frequency L-band EPR has circumvented these problems and *in vivo* EPR measurement is coming into use (4–11). In the EPR spin probe method, a paramagnetically stable spin probe, which is EPR-positive in stable conditions, is injected into the animals. This probe is reduced and loses its EPR signal in various organs, while measuring the EPR signal decay is equal to the measurement of organ reducing activity against a variety of radicals (5–7). As such, the measurement of spin probe-reducing activity by EPR may yield information about tissue radical reducing activity, redox status and biological status. Using *in vivo* EPR and EPR imaging technique (EPRI), we have previously succeeded with non-invasive evaluations of renal antioxidative status in various disease models (7, 9, 12, 13). We have improved the *in vivo* EPR application step-by-step in our previous reports and proved its accuracy for renal redox measurements. Since the invasiveness of EPRI is quite low, this method can be relevant to several aspects of pathophysiological or pharmacological investigations of oxidative stress research, including the evaluation of antioxidative or redox-related effects of drugs.

In this study, we applied EPRI for evaluating the oxidative stress of hypertension and the antioxidative effect of the antihypertensive reagent. Based on our fundamental studies, we applied *in vivo* EPR for the analysis of antioxidative activity of a calcium channel blocker (CCB), azelnidipine (Azl). CCBs inhibit the entry of calcium ions into vascular smooth muscle cells, which leads to vasodilation and a decrease in blood pressure. It is still under discussion whether antihypertensive drugs, including CCBs, have beneficial effects in preventing the major complications of hypertension, such as end-stage renal disease, through the control of oxidative stress (3). Among CCBs, Azl, a commercially available long-acting dihydropyridine-based calcium antagonist, is reported to possess an ability to reduce oxidative stress by several mechanisms (14–16). Although several reports have focused on various abilities of Azl or other CCBs in the control of hypertension, those reports were mainly *in vitro* or *ex vivo* studies, and *in vivo* real-time measurement of redox status during hypertensive therapy has been called for. In this study, in combination with *in vivo* EPR and EPRI, we imaged the antioxidative and reno-protective effect of Azl and succeeded in the application of *in vivo* EPR/EPRI for the evaluating tool for determining the drug's antioxidative capacities.

Methods

Hypertension Animal Model and Antihypertensive Treatment

A murine two kidney–one clip (2K1C) hypertension model was generated using 8-week-old male ICR mice by clipping

the right renal artery with a 0.12 mm gap-width clip according to a previously reported method (17). Animals were housed in temperature-controlled cages with day–night cycles and allowed free access to water *ad libitum*. Four weeks after the clipping procedure, blood pressures were checked, and mice with 130 mmHg or higher systolic blood pressure were used for these experiments. These 2K1C mice were divided into three groups: the hypertension group (HT) received no medication, the low-dose Azl group (Low Azl) was treated with 1 mg/kg/d of Azl, and the high-dose Azl group (High Azl) was treated with 3 mg/kg/d of Azl. Azl was administered orally as a sodium carboxy-methylcellulose (CMC) suspension. The HT group animals also received the same amount of CMC without Azl by the same method. Sham-operated mice, which underwent the same surgical procedure except for the clipping, served as controls.

Changes in serum creatinine and proteinuria in these mice were evaluated. The serum creatinine concentrations were measured by an automated analyzer. The urinary protein was measured by a commercially available protein quantification kit. The urine of each mouse was collected in a metabolic cage over a 24-h period.

The animal experiments were carried out in a humane manner after receiving approval from the Institutional Animal Experiment Committee of the University of Tsukuba and in accordance with the Regulation for Animal Experiments and with the Fundamental Guideline for Proper Conduct of Animal Experiment and Related Activities in Academic Research Institutions under the jurisdiction of the Ministry of Education, Culture, Sports, Science and Technology, Japan.

EPR Experimental Design

We employed two *in vivo* EPR techniques: an L-band EPR spectroscopy and EPRI. The L-band EPR spectroscopy measured the half-life of a nitroxide spin probe 3-carbamoyl-2,2,5,5-tetramethylpyrrolidine-1-oxyl (Carbamoyl-PROXYL) in the whole upper abdominal area, which provides accurate quantitative information. However, this half-life reflects the reducing activity not only of the kidney but of all upper abdominal organs, including the liver. EPRI provides information on Carbamoyl-PROXYL concentration in a specific localized area such as the kidney or liver. It needs approximately 240 s to obtain one comprehensible three-dimensional (3D) EPR image, and the maximum number of images is six in one Carbamoyl-PROXYL injection. Thus, EPRI should be treated as a semi-quantitative method.

In Vivo L-Band EPR Spectroscopy

Measurements with L-band EPR were conducted by a method previously reported (12). Briefly, Carbamoyl-PROXYL (300 mmol/L, 2 mL/kg) was injected into the mice through the tail vein 10 min after pentobarbital anesthesia. Each mouse was then placed in the EPR resonator with its upper abdominal

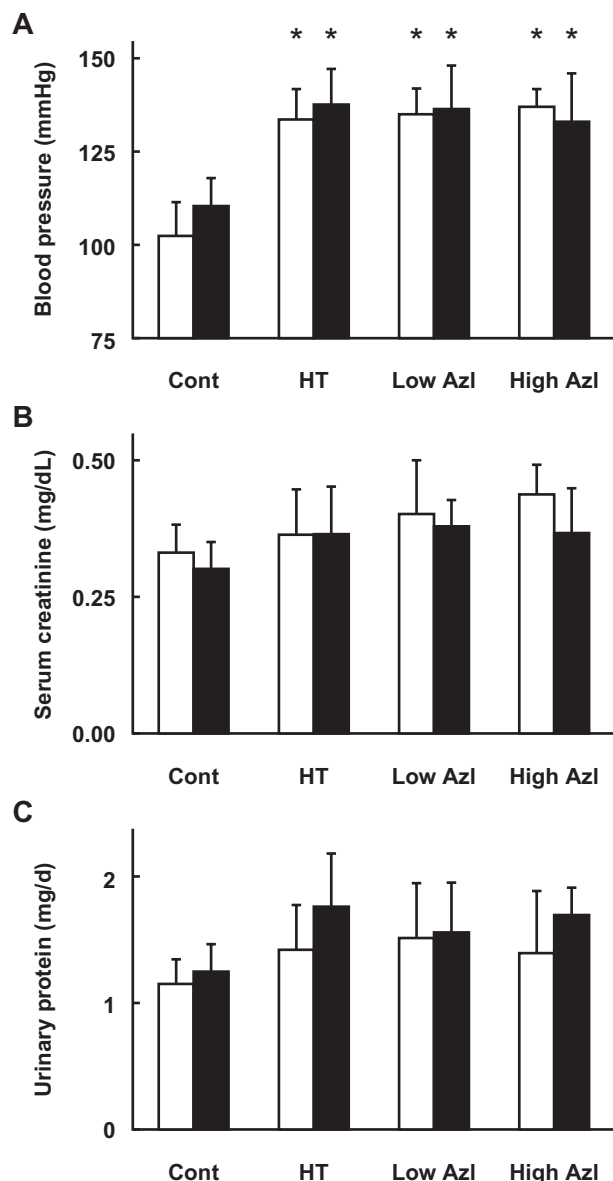


Fig. 1. Azelnidipine effects on blood pressure, serum creatinine and urinary protein in a murine 2K1C model. Blood pressure (A), serum creatinine (B) and urinary protein (C) of the HT, Low Azl and High Azl groups at the start (open columns) and week 2 (closed columns) are indicated. Significant increases in blood pressure were observed in the HT group during the observation period. * $p < 0.05$ vs. control.

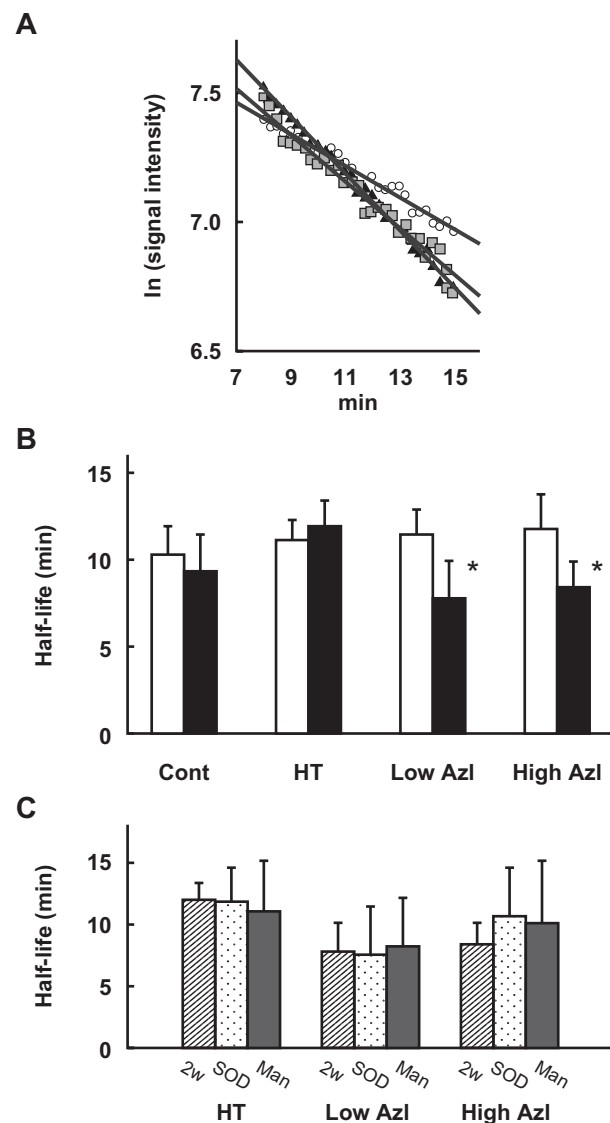


Fig. 2. L-band EPR spectroscopy measurement of the Carbamoyl-PROXYL half-life. A: Typical representative signal decay curves of Carbamoyl-PROXYL from HT (circles), Low Azl (triangles) and High Azl (squares) at week 2. The plot of signal intensities were fitted to a straight line on a semi-logarithmic scale, indicating that Carbamoyl-PROXYL reduction obeyed first-order kinetics during the time measured. B: Effects of azelnidipine on Carbamoyl-PROXYL half-lives in murine upper abdominal areas. Changes of the Carbamoyl-PROXYL half-life in HT ($n = 7$), Low Azl ($n = 6$) and High Azl ($n = 6$) before the observation periods (open columns) and week 2 (closed columns) are indicated. * $p < 0.05$ vs. HT at week 2. EPR conditions were described in Methods. C: Effects of radical scavengers on Carbamoyl-PROXYL half-lives. Changes of Carbamoyl-PROXYL half-lives at week 2 (hatched columns), after the addition of SOD (SOD: dotted columns) and mannitol (Man: gray columns) in HT, Low Azl and High Azl. Neither SOD nor mannitol had a significant effect on Carbamoyl-PROXYL half-lives ($n = 3$ each).

area in the center and the bladder outside. Rate constants (k) were calculated from the EPR signal intensities measured every 15 s from 8 to 14 min after the Carbamoyl-PROXYL injection. The half-life ($t_{1/2}$) was calculated using the equation $t_{1/2} = \ln 2/k$.

EPR Imaging

The detailed method for the measurement of organ-reducing activity by EPRI was established in our previous reports (7, 12). EPR images were obtained every 300 s until approximately 20 min after the Carbamoyl-PROXYL injection. EPR images were constructed by 3D zeugmatography using spectral data reconstructed by a filtered back projection (ESR-CT ver1.183 software; JEOL, Tokyo, Japan). On the obtained EPR images, a square area covering each organ was determined from the first image after the Carbamoyl-PROXYL injection. Similar to the L-band spectroscopy, the approximate first order spin reduction rate constant was estimated from the slope value of the observed clearance curve. The reducing activity was measured by the half-life of the signal intensities in each square area covering the corresponding organ.

EPR System and the Measuring Conditions

The L-band *in vivo* EPR/EPR imaging system used in this study consisted of a 1 GHz microwave unit and a bridged four-gap loop-gap resonator (38 mm diameter and 28 mm long, manufactured by JEOL). EPR conditions for these *in vivo* measurements were as follows: magnetic field, 37.0 ± 5.0 mT; modulation width, 0.69 mT; time constant, 0.03 s; microwave power, 0.25 mW; and microwave frequency, approximately 1,100 MHz. The conditions for EPRI were as follows: field gradient, 2.0 mT/cm; changing direction, 20 degree steps (provides eight spectra for each projection); magnetic field, 37.0 ± 5.0 mT; microwave power, 0.25 mW; modulation width, 0.1 mT; time constant, 0.1 s; scanning time for each spectrum, 30 s; and total scanning time, approximately 240 s.

Rule Out of EPR Signal Elimination by the Direct Oxidation of ROS

EPR signals of nitroxide radicals are also known to be eliminated by direct oxidation by specific ROS. To rule out this phenomenon, changes of the Carbamoyl-PROXYL half-life by the addition of a free radical specific scavenger were measured (12). Superoxide dismutase (SOD, 4 U/g) or mannitol was injected intravenously into the three groups of mice after 2 weeks of treatment. Soon after this injection, Carbamoyl-PROXYL was injected, and the half-life was measured using the *in vivo* L-band EPR system.

Statistical Analysis

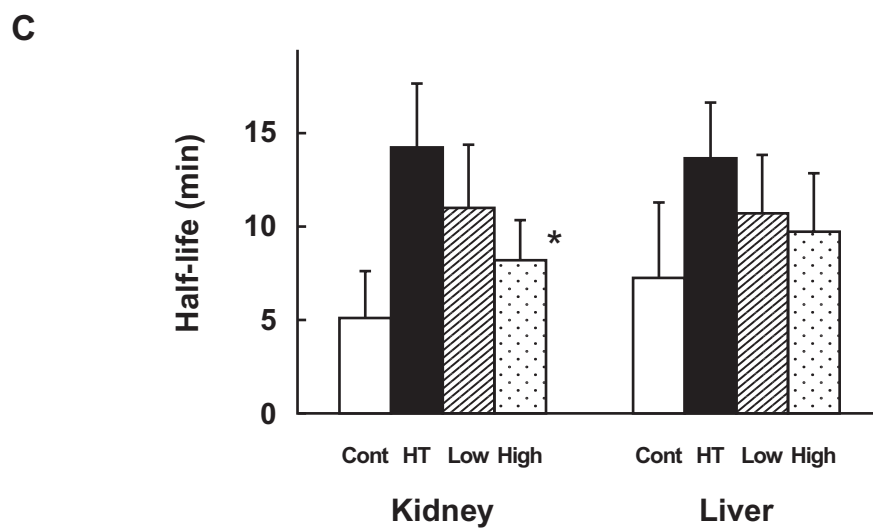
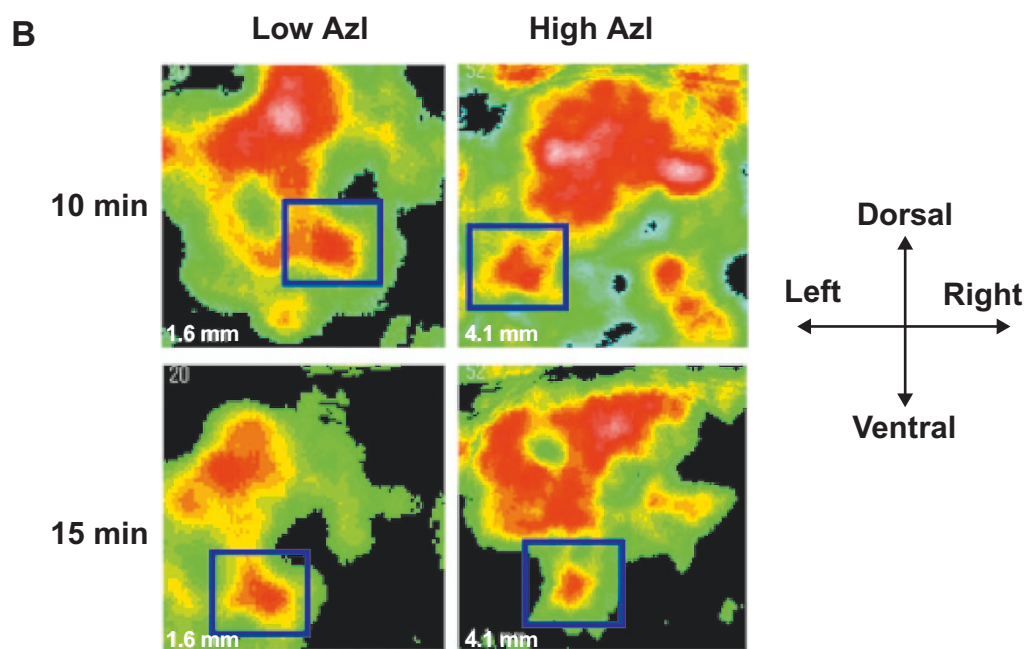
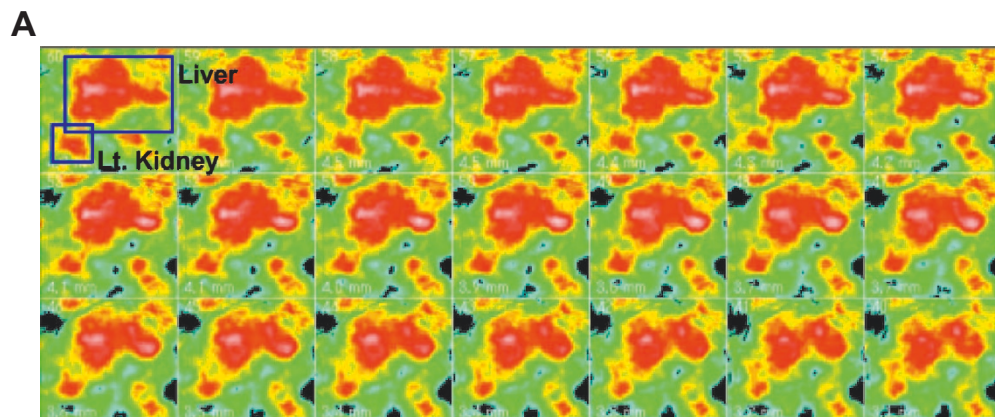
Significant differences between the groups of mice were analyzed by means of the analysis of variance with post hoc tests. Results are expressed as the means \pm SD.

Results

Azelnidipine Effects on Blood Pressure and Serum Creatinine in a Murine 2K1C Model

Blood pressure and heart rates were 102 ± 10 mmHg and 668 ± 69 bpm, respectively, in the untreated mice. Four weeks after the clipping procedure (before the start of the treatments), blood pressures were 133.6 ± 8.2 mmHg in HT ($n=10$), 134.6 ± 7.6 mmHg in Low Azl ($n=7$) and 136.7 ± 5.1 mmHg in High Azl ($n=9$), and there were no significant differences among the three groups (Fig. 1A). After the 2-week treatment period, the blood pressures were 137.6 ± 9.4 mmHg in the HT group, 136.1 ± 12.1 mmHg in Low Azl and 132.8 ± 13.3 mmHg in High Azl, and, again, no significant differences were observed. At the end of 4 weeks of treatment, the blood pressure of the HT group was 143.7 ± 8.5 mmHg. High Azl treatment significantly reduced blood pressure to 125.8 ± 7.6 mmHg. Low Azl also decreased BP to 134.9 ± 7.7 mmHg. However, this decrease was not significant.

Fig. 3. Renal and hepatic reducing activity measured by EPR imaging. A: Typical trans-axial EPR image of the murine upper abdominal area. A typical trans-axial 3D EPR image of the control mouse 10 min after the Carbamoyl-PROXYL injection is shown. High signal intensity is indicated in red and low intensity in blue. The tiled-image in the upper left corner is taken in the most cephalic section, and in the lower right corner is taken in the most caudal section of the abdomen. The blue square areas indicate the left renal and hepatic regions. EPR conditions are described in Methods. B: A typical series of EPR images of the upper abdomen at the 2nd week with Low and High Azl treatments. Images are shown at 10 min (upper) and 15 min (lower) after the Carbamoyl-PROXYL injection. The high-intensity area in the center of each tiled image represents the liver. The blue square areas reflect the left kidneys. These images faded away during the observation period due to tissue reduction against the nitroxide radical. The images of the right kidneys were unremarkable. C: EPRI-measured renal and hepatic reduction activity with Azl treatments. The half-lives of Carbamoyl-PROXYL at the renal and hepatic areas of control (open columns), HT (closed columns), Low Azl (hatched columns) and High Azl mice (dotted columns) at week 2 of the observation periods. The signal intensities are obtained from the image intensities (see Methods). The half-life of Carbamoyl-PROXYL decay is significantly prolonged on week 2 in both the kidney and the liver. In the kidney, the half-life was significantly improved with High Azl treatment. The hepatic reduction activities showed relatively minor improvements, with both Low and High Azl compared with those of kidneys. * $p < 0.05$ vs. HT.



The serum creatinine concentration was 0.33 ± 0.05 mg/dL in the untreated mice. These values were 0.38 ± 0.09 mg/dL in HT, 0.40 ± 0.10 mg/dL in Low Azl, and 0.42 ± 0.06 mg/dL in High Azl at the start of the observation period (Fig. 1B). Serum creatinine showed an increasing tendency in HT and a decreasing tendency in High Azl. However, neither of these was significant. The serum creatinine values of the HT, Low Azl and High Azl groups at 2 weeks were 0.36 ± 0.09 mg/dL, 0.38 ± 0.05 mg/dL and 0.36 ± 0.09 mg/dL, respectively, and, at 4 weeks they were 0.43 ± 0.06 mg/dL, 0.37 ± 0.05 mg/dL and 0.36 ± 0.06 mg/dL, respectively. The proteinuria of HT mice showed a higher tendency than that of Low and High Azl; however these were not statistically significant.

L-Band EPR Spectroscopy Revealed Blood Pressure-Independent Antioxidative Effects of Azelnidipine

Carbamoyl-PROXYL EPR signals were continuously observed until approximately 50 min after the injection (data not shown). In agreement with our previous studies (7, 12), the plots of signal intensities were fitted to a straight line on a semi-logarithmic scale indicating that *in vivo* Carbamoyl-PROXYL reduction obeyed first order kinetics during the time measured (typical signal decay curves are shown in Fig. 2A).

The half-life of Carbamoyl-PROXYL decay in the upper abdominal area of the control mice was 10.2 ± 1.7 min, and this did not remarkably change after 2 weeks: 9.2 ± 2.2 min. At the start of the observation period, the Carbamoyl-PROXYL half-lives were 11.2 ± 3.4 min in HT, 11.4 ± 1.4 min in Low Azl and 11.7 ± 1.4 min in High Azl, and there was no significant difference among the three groups. After 2 weeks of treatment, the half-life of the HT group lengthened to 11.9 ± 1.4 min. This value was improved in the Low and High Azl groups, for which the half-lives were 7.8 ± 2.1 min and 8.5 ± 1.7 min, respectively, and both were significantly shorter than that of the HT group ($p < 0.05$, Fig. 2B). At the end of 4 weeks of treatment, the half-lives lengthened to 14.7 ± 2.2 min in HT, 13.8 ± 2.3 min in Low Azl and 13.5 ± 3.5 min in High Azl. Single oral administrations of Azl (3 mg/kg) to control mice did not alter blood pressure (122 ± 6.3 mmHg before and 113 ± 8.6 mmHg after 6 h) or Carbamoyl-PROXYL half-lives within 6 h of treatment (8.7 ± 2.3 min before and 9.1 ± 3.6 min after 6 h).

These decreases of Carbamoyl-PROXYL half-lives at week 2 may have been brought about by improvement of organ reducing activity or increased free radical production (see Discussion). To distinguish these conflicting phenomenon, Carbamoyl-PROXYL signal intensities were measured with the simultaneous addition of SOD and mannitol. Neither scavenger changed the Carbamoyl-PROXYL half-lives significantly (Fig. 2C).

EPR Revealed an Improvement of Renal Antioxidative Activity by Azelnidipine

Because these results of *in vivo* EPR suggest that renal antioxidative activity deteriorated at week 4 (see Discussion), the EPR experiments were conducted mainly at week 2. Within 5 min of Carbamoyl-PROXYL injection, EPR-positive regions were observed in the upper abdomen in areas corresponding to the left kidney and the liver. A typical caudal EPR image of the abdominal area of a non-treated mouse is shown in Fig. 3A. The images of the clipped right kidney were typically smaller than those of the left kidney and agglutinated with the liver. The hepatic and renal distributions of Carbamoyl-PROXYL were confirmed by measuring the EPR signals in the homogenates of the corresponding organs (data not shown). Typical EPR images in the kidneys of Low and High Azl mice are shown in Fig. 3B. The half-lives of the kidney in the control mice, HT, Low Azl and High Azl were 5.0 ± 3.3 min, 14.2 ± 2.6 min, 10.9 ± 3.1 min and 8.2 ± 1.8 min, respectively, and Low and High Azl showed a significant decrease in the half-lives compared with those of the HT group. In the hepatic area, the half-lives in the control mouse, HT, Low Azl and High Azl were 7.2 ± 3.1 min, 13.6 ± 4.2 min, 10.8 ± 3.0 min and 9.7 ± 3.1 min, respectively, and Low Azl mice displayed shorter half-lives than those of the HT group, but the differences were not significantly different.

Discussion

Oxidative stress critically contributes to the pathogenesis of hypertension and its major complications, including nephrosclerosis and progressive renal failure (18–22). Besides the blood pressure is decreased by antihypertensive agents, the question of whether the antihypertensive reagents have a specific role in preventing the complications of hypertension, such as atherosclerosis and renal disease, both of which are related to oxidative stress, is a major issue in the study of this field (3). The antioxidative properties of CCBs are brought about by scavenging effects against ROS (23) or by the induction of intra- or extracellular antioxidative reactions. The former effect is brought by the specific structure of the dihydropyridine ring to eliminate unpaired electrons, and the latter is the outcome of antioxidative reactions such as increased endothelial NO production and reductions of angiotensin or endothelin (3, 24, 25). Azl is reported to suppress NADPH oxidase-mediated reactive oxygen species generation *via* its specific ability (26, 27). A recent report proved that the anti-atherosclerotic effect of Azl was independent of its blood pressure-lowering effects and brought about by the elimination of local oxidative stress and reduced expression of monocyte chemoattractant protein-1 and platelet-derived growth factor (16).

In our experiments Azl improved the prolongation of Carbamoyl-PROXYL. An accelerated EPR signal disappearance of nitroxyl spin probes, including Carbamoyl-PROXYL,

which consequently leads to a shortening of the half-lives, is brought about by two antithetical phenomena: an emphasized radical reducing activity and an increase in local ROS production (6, 10). Thus, the balance between the reducing activity of tissue and local free radical reactions determines the signal decay rate of nitroxyl radical spin probes. A previous report concerning SHR-SP rats revealed an increase in superoxide production, which leads to a shortening of the half-life of 3-methoxycarbonyl-2,2,5,5-tetramethylpyrrolidine-1-oxyl (MC-PROXYL), a lipophilic nitroxyl spin probe, in the rodent brain (28). In contrast to this, our experiments with SOD or mannitol resulted in no remarkable changes of Carbamoyl-PROXYL half-lives. Although the *in vivo* half-life of SOD is short, our method was sufficient to decrease the Carbamoyl-PROXYL half-life in a condition in which superoxide production is dominant (29, 30). In addition, the rate constant for the reaction between hydroxyl radicals and nitroxyl radicals is comparable to that of the reaction between hydroxyl radicals and mannitol (10). Therefore, in our results, the direct reactions between Carbamoyl-PROXYL and superoxide or the hydroxyl radical are less prominent and the change in the Carbamoyl-PROXYL half-life mainly reflects the reducing activity.

On the other hand, Carbamoyl-PROXYL is reported to be partially membrane-permeable and reflects both the extracellular (membrane surface) and the intracellular local redox status, where the former is predominant (31, 32). NAD(P)H oxidase located in vessels is considered to be the major source of ROS (18), and it may affect Carbamoyl-PROXYL half-lives. However, according to the above discussion, the changes of half-lives predominantly reflect antioxidative status but not the direct reactions between the spin probe and superoxide or other radicals produced in radical chain reactions. Thus, our results are interpreted such that Azl improved the reducing activity mainly on the endothelial or neighboring cells. This improvement may be brought about by an increase of intercellular antioxidants and/or a decrease of antioxidant consumption caused by decreased ROS. The cellular reducing activity against nitroxyl radicals is maintained by intracellular antioxidative molecules including glutathione (GSH) and ascorbates, especially by GSH (33, 34). GSH is also a key molecule in the bioreduction of nitroxide spin probes in the cellular or organelle level. It is known that the cellular biological status, such as proliferation, differentiation and apoptosis, correlates with changes in the half-cell reduction potential of the GSSG/2GSH couple (34). Therefore, our results of the shortening of the Carbamoyl-PROXYL half-lives at week 2 finally indicate improvements of renal redox status brought about by Azl, and these were independent of blood pressure control. The detailed mechanism for the intracellular alterations of antioxidants should be analyzed in further studies.

The interpretation of our results of Carbamoyl-PROXYL half-lives needs to be further discussed. First, there is a discrepancy between the results of EPR spectroscopy and EPRI at week 2, the former showing a diminution in Carbamoyl-

PROXYL half-lives on both Low and High Azl, whereas kidney EPRI showed an improvement only by High Azl. Our previous study revealed that EPR spectroscopy on an upper abdominal area reflects various internal redox-related events, including the reducing activity of the liver and non-related reactions such as urinary excretion of the probe, and EPRI is required to evaluate renal reducing activity (12). The current results reflect this same methodological limitation. Second, the half-lives were prolonged in all groups at week 4, suggesting deteriorated reducing activities. The change in Carbamoyl-PROXYL half-lives from shortening to prolongation due to the further progression of tissue redox damage has been reported in an acute phase of radiation-induced oxidative damage (6) as well as in the early stage of renal injury in a streptozotocin-induced diabetic model (35). We, also, observed this redox conversion in the current study. Finally, the alteration of Carbamoyl-PROXYL half-lives did not correlate with that of serum creatinine. This is explained by the fact that the reducing activity is independent of the glomerular filtration rate as proved in our previous report (12).

While various clinical trials have been conducted to control oxidative stress *via* antioxidant supplementations, a limited number have proved successful (36). One of the major reasons for this failure is the lack of adequate methods to identify the subjects who have an imbalance between ROS production and antioxidant defenses (19). The *in vivo*, real-time and non-invasive measurements of *in vivo* EPR and EPR imaging potentially meet this requirement. Our current study of EPRI/*in vivo* EPR provides a relevant and highly sensitive new method in the investigation of antioxidative or redox-related effects of drugs in hypertension research.

Acknowledgements

We thank Dr. Burton D. Cohen for his warm support for our study. We also thank Ms. Y. Shimozaawa and the members of Department of Nephrology, University of Tsukuba, for their assistance. Azelnidipine was provided by courtesy of Sankyo Co., Ltd.

References

- Halliwell B, Gutteridge JMC: Measurement of reactive species, in: Halliwell B, Gutteridge JMC (eds): Free Radicals in Biology and Medicine, 4th ed. London, Oxford Science Publications, 2007, pp 268–270.
- Dikalov S, Griendling KK, Harrison DG: Measurement of reactive oxygen species in cardiovascular studies. *Hypertension* 2007; **49**: 717–727.
- Godfraind T: Antioxidant effects and the therapeutic mode of action of calcium channel blockers in hypertension and atherosclerosis. *Philos Trans R Soc Lond B Biol Sci* 2005; **360**: 2259–2272.
- Yokoyama H, Lin Y, Itoh O, et al: EPR imaging for *in vivo* analysis of the half-life of a nitroxide radical in the hippocampus and cerebral cortex of rats after epileptic seizures. *Free Radic Biol Med* 1999; **27**: 442–448.

5. Togashi H, Matsuo T, Shinzawa H, *et al*: *Ex vivo* measurement of tissue distribution of a nitroxide radical after intravenous injection and its *in vivo* imaging using a rapid scan ESR-CT system. *Magn Reson Imaging* 2000; **18**: 151–156.
6. Miura Y, Ozawa T: Noninvasive study of radiation-induced oxidative damage using *in vivo* electron spin resonance. *Free Radic Biol Med* 2000; **28**: 854–859.
7. Hirayama A, Yoh K, Nagase S, *et al*: EPR imaging of reducing activity in Nrf2 transcriptional factor-deficient mice. *Free Radic Biol Med* 2003; **34**: 1236–1242.
8. Kuppusamy P, Li H, Ilangovan G, *et al*: Noninvasive imaging of tumor redox status and its modification by tissue glutathione levels. *Cancer Res* 2002; **62**: 307–312.
9. Ueda A, Nagase S, Yokoyama H, *et al*: Identification by an EPR technique of decreased mitochondrial reducing activity in puromycin aminonucleoside-induced nephrosis. *Free Radic Biol Med* 2002; **33**: 1082.
10. Utsumi H, Yamada K: *In vivo* electron spin resonance-computed tomography/nitroxyl probe technique for non-invasive analysis of oxidative injuries. *Arch Biochem Biophys* 2003; **416**: 1–8.
11. Yamada K, Yamamiya I, Utsumi H: *In vivo* detection of free radicals induced by diethylnitrosamine in rat liver tissue. *Free Radic Biol Med* 2006; **40**: 2040–2046.
12. Hirayama A, Nagase S, Ueda A, *et al*: *In vivo* imaging of oxidative stress in ischemia-reperfusion renal injury using electron paramagnetic resonance. *Am J Physiol Renal Physiol* 2005; **288**: F597–F603.
13. Ueda A, Yokoyama H, Nagase S, *et al*: *In vivo* temporal EPR imaging for estimating the kinetics of a nitroxide radical in the renal parenchyma and pelvis in rats. *Magn Reson Imaging* 2002; **20**: 77–82.
14. Matsui T, Yamagishi S, Nakamura K, Inoue H: Azelnidipine, a new long-acting calcium-channel blocker, inhibits tumour necrosis factor- α -induced monocyte chemoattractant protein-1 expression in endothelial cells. *J Int Med Res* 2006; **34**: 671–675.
15. Nakamura K, Yamagishi S, Inoue H: Unique atheroprotective property of azelnidipine, a dihydropyridine-based calcium antagonist. *Mel Hypotheses* 2005; **65**: 155–157.
16. Nakano K, Egashira K, Ohtani K, *et al*: Azelnidipine has anti-atherosclerotic effects independent of its blood pressure-lowering actions in monkeys and mice. *Atherosclerosis* 2008; **196**: 172–179.
17. Wiesel P, Mazzolai L, Nussberger J, Pedrazzini T: Two-kidney, one clip and one-kidney, one clip hypertension in mice. *Hypertension* 1997; **29**: 1025–1030.
18. Griendling KK, FitzGerald GA: Oxidative stress and cardiovascular injury. Part II: Animal and human studies. *Circulation* 2003; **108**: 2034–2040.
19. Papaharalambus CA, Griendling KK: Basic mechanisms of oxidative stress and reactive oxygen species in cardiovascular injury. *Trends Cardiovasc Med* 2007; **17**: 48–54.
20. Cifuentes ME, Pagano PJ: Targeting reactive oxygen species in hypertension. *Curr Opin Nephrol Hypertens* 2006; **15**: 179–186.
21. Taniyama Y, Griendling KK: Reactive oxygen species in the vasculature: molecular and cellular mechanisms. *Hypertension* 2003; **42**: 1075–1081.
22. Escobales N, Crespo MJ: Oxidative-nitrosative stress in hypertension. *Curr Vasc Pharmacol* 2005; **3**: 231–246.
23. Mason RP, Walter MF, Trumbore MW, Olmstead EG Jr, Mason PE: Membrane antioxidant effects of the charged dihydropyridine calcium antagonist amlodipine. *J Mol Cell Cardiol* 1999; **31**: 275–281.
24. Berkels R, Egink G, Marsen TA, Bartels H, Roesen R, Klaus W: Nifedipine increases endothelial nitric oxide bioavailability by antioxidative mechanisms. *Hypertension* 2001; **37**: 240–245.
25. Spieker LE, Flammer AJ, Lüscher TF: The vascular endothelium in hypertension. *Handb Exp Pharmacol* 2006; **176 Pt2**: 249–283.
26. Jinno T, Iwai M, Li Z, *et al*: Calcium channel blocker azelnidipine enhances vascular protective effects of AT1 receptor blocker olmesartan. *Hypertension* 2004; **43**: 263–269.
27. Yamagishi S, Inagaki Y, Nakamura K, Imaizumi T: Azelnidipine, a newly developed long-acting calcium antagonist, inhibits tumor necrosis factor- α -induced interleukin-8 expression in endothelial cells through its anti-oxidative properties. *J Cardiovasc Pharmacol* 2004; **43**: 724–730.
28. Lee MC, Shoji H, Miyazaki H, *et al*: Assessment of oxidative stress in the spontaneously hypertensive rat brain using electron spin resonance (ESR) imaging and *in vivo* L-band ESR. *Hypertens Res* 2004; **27**: 485–492.
29. Sano T, Umeda F, Hashimoto T, Nawata H, Utsumi H: Oxidative stress measurement by *in vivo* electron spin resonance spectroscopy in rats with streptozotocin-induced diabetes. *Diabetologia* 1998; **41**: 1355–1360.
30. Han JY, Takeshita K, Utsumi H: Noninvasive detection of hydroxyl radical generation in lung by diesel exhaust particles. *Free Radic Biol Med* 2001; **30**: 516–525.
31. Okajo A, Matsumoto K, Mitchell JB, Krishna MC, Endo K: Competition of nitroxyl contrast agents as an *in vivo* tissue redox probe: comparison of pharmacokinetics by the bile flow monitoring (BFM) and blood circulating monitoring (BCM) methods using X-band EPR and simulation of decay profiles. *Magn Reson Med* 2006; **56**: 422–431.
32. Yamada K, Inoue D, Matsumoto S, Utsumi H: *In vivo* measurement of redox status in streptozotocin-induced diabetic rat using targeted nitroxyl probes. *Antioxid Redox Signal* 2004; **6**: 605–611.
33. Fuchs J, Groth N, Herrling T, Zimmer G: Electron paramagnetic resonance studies on nitroxide radical 2,2,5,5-tetramethyl-4-piperidin-1-oxyl (TEMPO) redox reactions in human skin. *Free Radic Biol Med* 1997; **22**: 967–976.
34. Schafer FQ, Buettner GR: Redox environment of the cell as viewed through the redox state of the glutathione disulfide/glutathione couple. *Free Radic Biol Med* 2001; **30**: 1191–1212.
35. Hirayama A, Yoh K, Ueda A, *et al*: Nrf2 deficiency intensifies early phase renal damage in streptozotocin-induced diabetic mice. *Free Radic Biol Med* 2004; **37**: S134.
36. Bjelakovic G, Nikolova D, Gluud LL, Simonetti RG, Gluud C: Mortality in randomized trials of antioxidant supplements for primary and secondary prevention: systematic review and meta-analysis. *JAMA* 2007; **297**: 842–857.